Preliminary Investigation: 2D-3D Registration of MR and X-ray Cardiac Images Using Catheter Constraints

Michael V.N. Truong, Abdullah Aslam, Christopher Aldo Rinaldi, Reza Razavi, Graeme P. Penney, Kawal Rhode

Preliminary Investigation: 2D-3D Registration of MR and X-ray Cardiac Images Using Catheter Constraints

Michael VN Truong[1], Abdullah Aslam[1], C Aldo Rinaldi[2], Reza Razavi[1], Graeme P Penney[1] and Kawal S Rhode[1]

[1] Division of Imaging Sciences, King's College London, UK; [2] Department of Cardiology, Guy's & St. Thomas' Hospitals NHS Foundation Trust, UK
{michael.truong, abdullah.aslam}@kcl.ac.uk, aldo.rinaldi@gstt.nhs.uk, {reza.razavi, graeme.penney, kawal.rhode}@kcl.ac.uk

Abstract. Cardiac catheterization procedures are routinely guided by X-ray fluoroscopy but suffer from poor soft-tissue contrast and a lack of depth information. These procedures often employ pre-operative magnetic resonance or computed tomography imaging for treatment planning due to their excellent soft-tissue contrast and 3D imaging capabilities. We developed a 2D-3D image registration method to consolidate the advantages of both modalities by overlaying the 3D images onto the X-ray. Our method uses electrophysiology catheters that are typically placed in vessels of the heart where they remain throughout the procedure. Vessels were segmented from the 3D anatomical scans, and the 3D catheter positions were reconstructed from sequential biplane X-ray image pairs. To achieve registration, an automatic global-fit algorithm was developed which minimized the RMS distance error of the catheter to the medial line of its respective vessel. Data were processed for two clinical cases and an accurate registration was validated by visual inspection.

Keywords. 2D-3D image registration, cardiac imaging, image guided catheterization, MR, CT, X-ray

1 Introduction

Cardiac catheterization procedures are routinely guided using X-ray fluoroscopy. This modality is suitable due to its high spatial and temporal resolutions, relative low-cost, ubiquitous availability and excellent catheter visibility. However, fluoroscopy has poor soft-tissue contrast and the cardiologists need to rely on their expertise to accurately position the catheters. Cardiac electrophysiology (EP) procedures are commonly carried out to treat electrical pathologies, such as arrhythmias, usually using radio-frequency (RF) ablation of endocardial tissue. These procedures are often prolonged due to the requirement of accurate positioning of catheters and therefore there is significant radiation exposure to the patient and staff, and often a suboptimal success rate. Recently, there has been much research to register pre-procedural three-dimensional (3D) anatomical information from computerized tomography (CT) or magnetic resonance (MR) imaging to help guide EP procedures by overlaying the 3D anatomical information onto the live two-dimensional (2D) X-ray fluoroscopy [1].

Rhode *et al*. previously reported a technique that uses a pre-calibrated hybrid X-ray/MR (XMR) imaging system [2]. However, these systems are not widely available outside the research environment. 2D-3D registration for these procedures can be carried out using surrogate structures such as fiducial skin markers [3, 4, 5], photogrammetry systems [6], and the spine [7]. However, the relative motion between the heart and the surrogates due to cardiac and respiratory motion may compromise their accuracy, and surrogates must always be in the same field of view as the heart in order to perform registration; these would not be an issue if the target organ is used itself. Approaches that do so include manual registration with biplane contrast-filled angiograms [8, 9] and using the catheter that is placed within the coronary sinus (CS) during EP procedures (EPNavigator, Philips Healthcare).

Using the CS catheter for registration is attractive since no additional data acquisition is required and therefore there is no disturbance to the routine clinical workflow. Sra *et al.* first proposed using the CS catheter for 2D-3D registration [10]. In this approach, a catheter was placed in the CS via the superior vena cava (SVC). The CS and the SVC were segmented from CT data and then used to align the data to a single X-ray projection of the CS catheter. The patient was assumed to lie in a similar manner on both the CT and X-ray table during imaging so that the scaling parameters of the X-ray system could be approximated. This registration would have to be performed every time the X-ray c-arm or patient table was moved. Furthermore, the authors reported that manual adjustment of registration was required in nine out of 20 of the reported clinical cases.

We aim to develop a clinically robust method to perform 2D-3D registration of 3D cardiac data (CT or MR) to X-ray fluoroscopy data using catheters that are reconstructed in 3D from sequential biplane X-ray images, and structures segmented from 3D MR data. We focus on the use of the CS and the aortic catheters. Our approach differs from that of Sra *et al.* because we perform the registration in 3D and then project to the X-ray imaging plane using a pre-calibration of the X-ray system. Furthermore, the registration only needs to be performed at the beginning of the procedure and is then updated automatically by tracking the motion of the X-ray c-arm and table. A repeat registration is only required if the patient has moved on the X-ray table. We demonstrate the use of the approach on a clinical EP procedure.

2 Method

The clinical procedures were performed in the XMR interventional suite at St. Thomas' Hospital, London, which is equipped with a 1.5T cylindrical bore MR scanner (Achieva, Philips Healthcare) and a single plane X-ray system (BV Pulsera, Philips Healthcare). The X-ray system projection geometry was pre-calibrated and the c-arm and patient table were tracked [2]. Two patients with heart failure were imaged under MR and underwent a pacing study prior to pacemaker implantation. The imaging used a whole heart MR sequence carried out after the administration of a blood pool contrast agent (Vasovist, Bayer Schering Pharma). The sequence was a

3D steady-state free precession scan with an inversion recovery preparation RF-pulse, respiratory navigator gated at end-expiration and ECG triggered at late diastole. During the EP procedure, the CS was catheterized followed by the acquisition of sequential biplane fluoroscopy images at ten frames per second during free-breathing. While the procedures were performed in an XMR suite, its automatic X-ray to MR registration capabilities were not utilized for our method. In conventional cath-labs settings, our method of registration would be equally applicable as long as the X-ray c-arm's orientation is tracked.

2.1 Registration Workflow

The workflow of our registration is divided into three stages. The MR stage involves the extraction of the medial line of the CS. The X-ray stage involves the 3D reconstruction of the CS catheter. Lastly, in the registration stage, we find a transformation that minimizes the root mean square (RMS) distance error between the medial line of the CS and the catheter reconstruction. This transformation, combined with the calibrated and tracked X-ray system, enables us to perform the overall 2D-3D registration.

2.2 Extraction and Skeletonization of the Coronary Sinus from MRI

The interactive segmentation of the CS from the MR scan was carried out using a specially modified version of ViewForum (Philips Healthcare) (Fig. 1a). Since the CS is much longer than it is thick, we approximate it to its medial line. The initial medial line was found using a 3D 6-subiteration curve thinning algorithm [11] but it was sensitive to imaging and segmentation artifacts resulting in extraneous branches, internally-closed circuits (ICC) and large nodes (LN) (Fig. 1b). Therefore we employed a combination of image processing techniques to clean up the skeleton [12], first applying consecutively an erosion and dilation to the pre-skeletonized segmented volume. We then convolved the skeleton with a 3×3×3 Gaussian kernel and reapplied the skeletonization to remove the ICCs and LNs. Finally, we removed any short branches from the remaining skeleton. This two-pass thinning process produced a cleaner and simpler skeleton while maintaining the rough topology of the segmented CS (compare fig.1b, 1c).

Geometrically the catheter is homeomorphic to a line and thus may only be contained by one distinct pathway within the skeleton (Fig 1c). While manual selection of the containing pathway is a viable solution, an algorithm capable of finding it without user interaction is a better one. Therefore, our algorithm considers every possible pathway of the skeleton. Furthermore, for each pathway is another consisting of the same points but with reverse ordering and must also be considered in our algorithm.

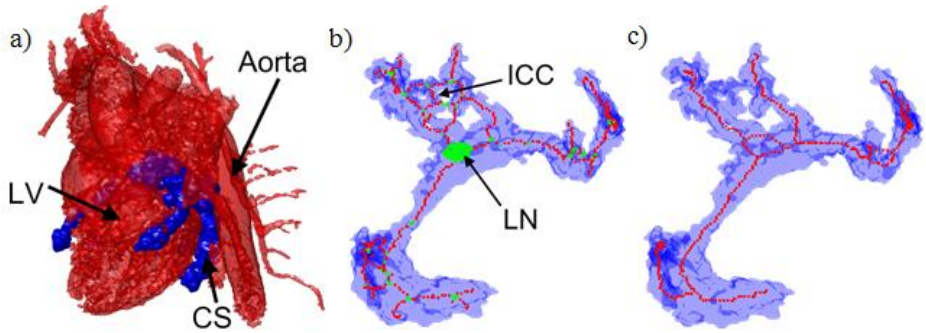

Figure 1. a) The coronary sinus (*blue, labeled CS*) segmented from the rest of the heart (*red, translucent*). The left ventricle (*LV*) and aorta are labeled. b) The coronary sinus (*blue, translucent*) and its skeleton, divided into branches (*red, opaque*) and nodes (*green, opaque*). 1202 distinct pathways can be produced from this skeleton. c) Skeleton after cleaning (*red, opaque*) drawn within the segmented CS (*blue, translucent*); only 80 distinct pathways remain.

2.3 Coronary Sinus Catheter from X-ray

We reconstruct the CS catheter in 3D using epipolar geometry [13] from cardiac and respiratory gated X-ray images. This first requires that we calibrate our X-ray c-arm and we do so using the methods described in [2] to obtain the x-ray system's *intrinsic* parameters. With these parameters and a tracked c-arm system, we manually selected the points from the catheter in the left image and then selected the corresponding points in the right image using the epipolar constraint (Fig 2). Once the set of corresponding points are collected from both images, they are back-projected to yield its corresponding location in the 3D coordinate system of the X-ray table (table coordinate system).

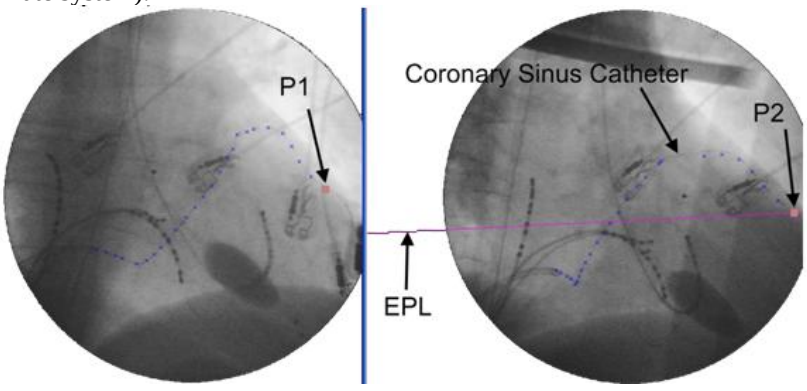

Figure 2. Two views of a heart gated at end-diastole and end-expiration taken at AP (*left*) and LAO 60° (*right*). Points along the CS catheter are selected in both images (*blue crosses*). A point from the left image (*P1*) will generate an epipolar line in the right image (*EPL*). P1's corresponding point will lie at an intersection of this line and the catheter (*P2*).

2.4 Registration

Registration of our MR and X-ray images requires that we find the relationship between the patient's positions while he or she is lying in the MR scanner, and when lying on the X-ray table. Since the images acquired are cardiac and respiratory gated in both imaging modalities, we assume that the heart returns to the same shape at the same phase, and therefore describe this relationship as a *rigid-body transformation* which can be represented as $\mathcal{T} = (R, \vec{r}_0)$, with

$$\vec{r}_{t,i} = R\vec{r}_{s,i} + \vec{r}_0 + e_i;\ \forall\, i \in [1, n] \qquad (1)$$

Where $\{\vec{r}_{t,i}\}$ is the set of points in the table coordinate system and $\{\vec{r}_{s,i}\}$ is the set of corresponding points in the MR scanner coordinate system, R is the 3×3 rotation matrix, and $\vec{r}_0$ is the translation vector. The residual error of this transformation is denoted as e, and is calculated by Eq. 2. By representing the transformation in this form, it readily identifies itself as the Orthogonal Procrustes problem [14].

$$e = e(\vec{r}_s, \vec{r}_t) = \frac{1}{n}\sum_{i=1}^{n} \|e_i\|^2 = \frac{1}{n}\sum_{i=1}^{n} \left\|\left(R\vec{r}_{s,i} + \vec{r}_0\right) - \vec{r}_{t,i}\right\|^2 \qquad (2)$$

The solution requires that we have a point-to-point correspondence between our catheter defined in the table coordinate system, and the CS defined in the scanner coordinate system. However, this correspondence does not exist since neither the set of catheter points obtained by 3D reconstruction from two X-ray views, nor the collection of points that make up the skeletonization pathways of the CS are uniformly sampled. To remedy this, we fit a natural cubic spline through the set of catheter points and sample it at 0.2 mm intervals to produce a new set of evenly sampled points for the catheter (catheter curve), and do the same for each set of CS points (CS curves). The new evenly sampled points are used with the Procrustes solution. The following global-fit pseudo-code algorithm determines which of the CS curves, when compared against the catheter curve, would yield the lowest error.

```
Let rt[i] be the i-th point of the catheter curve
Let rs[k][i] be the i-th point of the k-th CS curve
Let r[a:b] be the subcurve of r between a and b.
for k = 1 to # of CS curves
  n = # of points in rt; m = # of points in rs[k]
  L = max(m, n) - min(m, n) + 1
  if n > m: I = argmin{i}(e(rs[k][1:n], rt[i:i+L-1])),
            E[k] = e(rs[k][1:n], rt[I:I+L-1]);
  else: I = argmin{i}(e(rs[k][i:i+L-1], rt[1:m])),
        E[k] = e(rs[k][I:I+L-1], rt[1:m]);
return argmin{k}(E[k])
```

Once we find the transformation that yields the minimum residual error, the 2D-3D registration can be performed by applying the transformation to the MR image of the heart and projecting it onto the X-ray images.

2.5 Registration using Multiple Catheter/Vessel Pairs

A potential problem with relying on a single catheter/vessel pair occurs if they do not have sufficient curvature. As an illustrative example, if both the catheter and its containing vessel were straight, then the catheter may slide along the axis of the vessel without a change in the calculated residual error. Additionally, in our algorithm that compares the CS catheter to every possible path of the CS, it is possible that two or more paths may have a very similar shape to the catheter, yielding competitively low residual errors. Both these degenerate scenarios may be improved by introducing an additional catheter that is constrained to lie in a vessel throughout the procedure, such as the one lying in the aorta. A drawback to using the aorta, or other vascular structures with a large diameter, is that the catheter has more room to move around, thus the assumption that catheter lies close to its medial line is less likely to be correct. However, the gain in accuracy of introducing a second catheter/vessel pair should outweigh any potential reductions in accuracy caused by the catheter lying a distance from the vessel's medial line.

3 Results

For our 2D-3D algorithm, we consider two clinical cases where cardiac catherization was performed and show example results from one of these cases. Following the method outlined above, the coronary sinus was extracted from the heart and skeletonised (Fig. 1). Extraction by an expert could be performed in under 30 minutes, and the two-pass skeletonization requires one hour to compute (Intel Core 2 Extreme @ 2 × 3.07 GHz, 4 GB RAM). The catheter was also reconstructed in 3D by selected points from sequential biplane images (Fig. 2). The manual selection of the catheter from both projection views by an expert could be performed in under 20 minutes. Approaches to automate and speed up the extraction of the catheter and vessels are addressed in the discussion section.

The reconstruction of the catheter in 3D, fitted with a cubic spline is shown in Fig. 3a. An example residual error curve is shown in Fig. 3b where, for a particular CS curve, the Procrustes solution is applied using its subcurves and the catheter curves. We choose the transformation that yields the lowest residual error for our registration. The dual catheter equivalent of the residual curve is a residual surface (Fig. 3c) where all combinations of the CS curves with the CS catheter, and the aorta curves with the aortic catheter, must be explored.

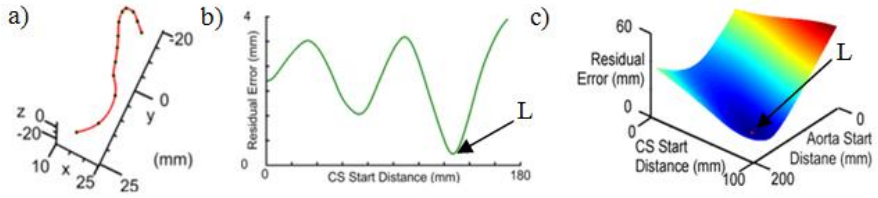

Figure 3. a) The catheter points are reconstructed in 3D and a spline is fitted through them. b) For each CS curve, the Procrustes solution is applied between its subcurves and the catheter curve. The lowest point (*labeled L)* indicates where the catheter starts along the particular CS curve. Only one pathway is shown; there would be 80 if using the skeleton from Fig. 1c. c) The two catheter equivalent of b); the minimum is at the valley of the surface (*labeled L)*

In Fig. 4a we apply our transformation on the segmented coronary sinus image and draw the catheter onto the image. Once we find the transformation to get the image into the table coordinate system, we may apply it to the 3D image of the heart using Eq. 1, then use the intrinsic parameters to project it onto one of the intraoperative X-ray images as in Fig. 4b and c. While our algorithm was able to find an accurate registration for one case, it was unsuccessful when applied to the second. We found that the geometric relationship between the CS and aorta from MR did not match the relationship between the reconstructed CS and aortic catheters from X-ray, resulting in a misaligned registration. This is discussed further in the next section. The global-fit registration algorithm for a single catheter could be performed in 25 minutes, while the dual catheter registration's computation time was significant at 30.8 hours.

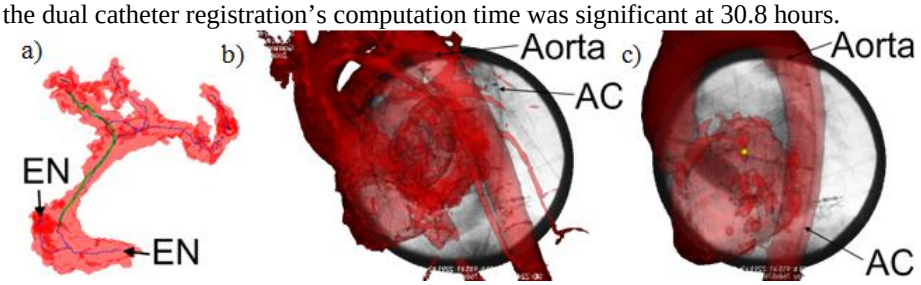

Figure 4. a) The CS (*red, translucent*) in the table coordinate system using the transformation found, with the skeleton (*blue*) and the catheter (*green*). The catheter may have entered from either points labeled *EN*. b) A model of the heart (*red, translucent*) overlaid on top of the intraoperative x-ray image using only the CS to constrain the registration. The segment of the aortic catheter (*labeled AC*) does not lie in the segment of the aorta. c) as b), except using both the CS and aortic catheter/vessel pairs, resulting in a more accurate registration.

4 Discussion and Conclusion

We have shown that we can accurately perform a 2D-3D registration algorithm to achieve an overlay of preoperative MR image on top of the intraoperative X-ray using data from routine clinical cases. The algorithm relies on catheters placed within vessels that remain there throughout the procedure. In cardiac catheterisation

procedures, this is a valid assumption as it is typical to employ several such catheters to collect essential EP data from the patient.

Our method also uses the rigid-body assumption; that the heart is the same shape for all images taken both end-diastole and end-respiration. However, the heart is a non-rigid structure that undergoes significant motion and deformation over the respiratory and cardiac cycles. Since our MR and X-ray images used for registration are acquired with many cardiac and respiratory cycles between them, this assumption may be compromised. A small improvement can be made by using simultaneous biplane, as show in [15] however a biplane X-ray system is required and this is not widely used for EP procedures. Additionally, the catheters are relatively rigid compared to the heart, and we believe that a catheter resting in a vessel may deform it during the procedure compared to when the 3D images are acquired. Therefore, we believe that the deformability of the heart is a primary contributing factor to the error of our registration and is likely the cause of failure in our second case. On the other hand, hereto this paper, we have only considered using two of these catheters for registration and we have yet to determine if the inclusion of a third catheter may increase accuracy, precision, or provide redundancy and hence robustness; albeit at the expense of a longer computational time.

The computational cost of our algorithm is a concern since it is intended to be employed intra-operatively; once for the initial registration of the heart and for each time there is bulk patient motion. A future improvement to reduce computing time would be to adaptively sample the catheter and vessel splines – initially at a courser resolution to narrow down the number of potential vessel pathway candidates, then at the finer resolution of 0.2 mm as per the current algorithm on the remaining candidates. Additionally, our algorithm would benefit greatly from using parallel and GPU processing since most of the computations may be performed independently of each other due to the global-fit nature of our approach. Lastly, our method requires the manual extraction of the catheters in X-ray and of the corresponding vessel in MR, which adds to the overall processing time. In the future, we envision our algorithm to be completely automated, potentially by employing the techniques presented in [13] for automatic catheter extraction from a biplane X-ray pair, in [16] for automatic segmentation in MR and in [17] for CT.

While our results are still preliminary, we believe that our 2D-3D registration algorithm, combined with a tracked c-arm for real-time capabilities, may improve the visualization of catheter interventions guided under fluoroscopy.

References

1. Sra, J., Ratnakumar, S.: Cardiac image registration of the left atrium and pulmonary veins. Heart Rhythm 5(4), 609--617 (Apr 2008); Epub (2007 Dec 5)
2. Rhode, K.S., Sermesant, M., Brogan, D., Hegde, S., Hipwell, J., Lambiase, P., Rosenthal, E., Bucknall, C., Qureshi, S.A., Gill, J.S., Rezavi, R., Hill, D.L.G.: A System for Real-Time

XMR Guided Cardiovascular Intervention. IEEE Trans. Med. Imag. 24(11), 1428--1440 (2005 Nov)

3. de Silva, R., Gutiérrez, L.F., Raval, A.N., McVeigh, E.R., Ozturk, C., Lederman, R.J.: X-ray fused with magnetic resonance imaging (XFM) to target endomyocardial injections: validation in a swine model of myocardial infarction. Circulation, 114(22), 2342--2350 (2006 Nov); Epub (2006 Nov 13)
4. Gutiérrez, L.F., de Silva, R., Ozturk, C., Sonmez, M., Stine, A.M., Raval, A.N., Raman, V.K., Sachdev, V., Aviles, R.J., Waclawiw, M.A., McVeigh, E.R., Lederman, R.J.: X-Ray Fused With Magnetic Resonance During Invasive Cardiovascular Procedures. Catheterization and cardiovascular Interventions 70, 773--782 (2007)
5. Rhode, K., Ma, Y., Chandrasena, A., King, A., Gao, G., Chinchapatnam, P., Sermesant, M., Hawkes, D., Schaeffter, T., Gill, J., Razavi, R.: Evaluation of the use of multimodality skin markers for the registration of pre-procedure cardiac MR images and intra-procedure x-ray fluoroscopy images for image guided cardiac electrophysiology procedures. Proc. SPIE 6918 (2008)
6. Gao, G., Tarte, S., King, A., Ma, Y., Chinchapatnam, P., Schaeffter, T., Razavi, R., Hawkes, D., Hill, D., Rhode, K.: Validation of the use of photogrammetry to register pre-procedure MR images to intra-procedure patient position for image-guided cardiac catheterization procedures. Proc. SPIE 6918 (2008)
7. Penney, G.P., Batchelor, P.G., Hill D.L., Hawkes D.J., Weese, J.: Validation of a two- to three-dimensional registration algorithm for aligning preoperative CT images and intraoperative fluoroscopy images. Med. Phys. 28(6), 1024-1032 (2001 Jun)
8. Ector J., De Buck, S., Adams, J., Dymarkowski, S., Bogaert, J., Maes, F., Heidbüchel, H.: Cardiac three-dimensional magnetic resonance imaging and fluoroscopy merging: a new approach for electroanatomic mapping to assist catheter ablation. Circulation 112(24), 3769--3776 (2005 Dec); Epub. (2205 Dec 5)
9. Ector, J., De Buck, S., Huybrechts, W., Nuyens, D., Dymarkowski, S., Bogaert, J., Maes, F., Heidbüchel, H.: Biplane three-dimensional augmented fluoroscopy as single navigation tool for ablation of atrial fibrillation: accuracy and clinical value. Heart Rhythm 5(7), 957-964 (2008 Jul); Epub. (2008 Mar 25)
10. Sra, J., Krum, D., Belanger, B., Vaillant, R.: Registration of three-dimensional left atrial computed tomographic images with fluoroscopy. Heart Rhythm 2(9), 1020 (Sep 2005)
11. Lohou, C., Bertrand, G.: A 3D 6-subiteration curve thinning algorithm based on P-simple points. Disc. Appl. Math. 151, 198--228 (2005)
12. Gonzalez, R.C., Woods, R.E.: Digital Image Processing, 2nd Ed. Prentice-Hall, Inc.; Upper Saddle River, New Jersey (2002)
13. Baert, S.A.M., van de Kraats, E.B., van Walsum, T., Viergever, M.A., Niessen, W.J.: Three-Dimensional Guide-Wire Reconstruction From Biplane Image Sequences for Integrated Display in 3-D Vasculature. IEEE Trans. Med. Imag., 22(10), 1252--1258. (2003 Oct)
14. Schönemann, P.H., A generalized solution of the orthogonal Procrustes problem. Psychometrika 31, 1--10 (1966)
15. Pathak, C., van Horn, M., Weeks, S., Bullitt, E.: Comparison of Simultaneous and Sequential Two-View Registration for 3D/2D Registration of Vascular Images. In: Duncan, J.S., Gerig, G. (eds.) MICCAI 2005. LNCS, vol. 3750, pp. 239--246. Springer (2005)
16. Peters, J., Ecabert, O., Meyer, C., Schramm, H., Kneser, R., Groth, A., Weese, J.: Automatic Whole Heart Segmentation in Static Magnetic Resonance Image Volumes. In: Ayache, N., Ourselin, S., Maeder, A., (eds.) MICCAI 2007. LNCS, vol. 4792, pp. 402--410. Springer (2007)
17. Ecabert, O., Peters, J., Schramm, H., Lorenz, C., von Berg, J., Walker, W.J., Vembar, M., Olszewski, M.E., Subramanyan, K., Lavi, G., Weese, J.: Automatic Model-Based Segmentation of the Heart in CT Images. IEEE Trans. Med. Imag. 27(9), 1189--1201 (2008 Sep)